

Primers for the Adhesion of Gellan Gum-Based Hydrogels to the Cartilage: A Comparative Study

Diego Trucco,* Laura Riacci, Lorenzo Vannozzi, Cristina Manferdini, Lorenzo Arrico, Elena Gabusi, Gina Lisignoli, and Leonardo Ricotti

A stable adhesion to the cartilage is a crucial requisite for hydrogels used for cartilage regeneration. Indeed, a weak interface between the tissue and the implanted material may produce a premature detachment and thus the failure of the regeneration processes. Fibrin glue, cellulose nanofibers and catecholamines have been proposed in the state-of-the-art as primers to improve the adhesion. However, no studies focused on a systematic comparison of their performance. This work aims to evaluate the adhesion strength between *ex vivo* cartilage specimens and polysaccharide hydrogels (gellan gum and methacrylated gellan gum), by applying the mentioned primers as intermediate layer. Results show that the fibrin glue and the cellulose nanofibers improve the adhesion strength, while catecholamines do not guarantee reaching a clinically acceptable value. Stem cells embedded in gellan gum hydrogels reduce the adhesion strength when fibrin glue is used as a primer, being anyhow still sufficient for *in vivo* applications.

cell survival and proliferation framework. Besides, the possibility to deliver them in the articular cavity through minimally invasive procedures to match irregular defects makes hydrogels promising for substitution or regenerating damaged articular cartilage after traumas or degenerative pathologies. In both cases, integrating hydrogels and surrounding tissues is crucial to restore the native properties (e.g., mechanical ones) and promote healing processes.^[7] Indeed, a weak integration may produce possible detachment over time, a sub-optimal transmission of mechanical loads and other undesired phenomena ultimately leading to the failure of cartilage substitution or regeneration objective.^[8]

At present, the achievement of a stable and durable hydrogel adhesion after its deposition onto the native articular cartilage

1. Introduction

Injectable or *in situ* crosslinked hydrogels for cartilage tissue engineering constitute a hot topic in the field of orthopedics.^[1–6] Hydrogels are based on three-dimensional networks of polymeric chains featured by high water content. They have similarities with the natural extracellular matrix (ECM), constituting a porous


tissue represents an often-neglected problem. Especially when dealing with soft and deformable hydrogels, the investigation of the adhesion strength between the cartilage and the deposited material is of utmost importance to guarantee that the biomaterial safely remains in the target region, providing its stimuli (either due to the own material properties or to the cells embedded in it) at a local level.^[9] The use of adhesive primers can be used for this purpose. An adhesive primer, or adhesion promoter, consists of a coating applied to a surface to promote the adhesion of other materials on it. The medical adhesives used in orthopedics (e.g., cyanoacrylates) usually employed in the clinics show relatively some disadvantages, thus joint brittleness, gap curing limitation, poor solvent and temperature resistance and stress cracking may occur if bonded with some polymers resulting in low performances and weak tissue adhesion. This aspect deserves attention and dedicated studies.

Different strategies have been proposed to address this challenge.^[10,11] Among them, the use of fibrin glue (FG), cellulose nanofibers (CNFs) or catecholamines (CATs) may constitute a promising route to be pursued. FG is a surgical glue typically used in the clinic to create a fibrin clot for hemostasis or wound healing. It has been investigated both as a cell-laden hydrogel for cartilage tissue engineering^[12] or as a primer to promote the adhesion of other materials on the cartilage surface.^[13] Some aspects related to FG crosslinking have been studied in the past years (e.g., the difference between commercial formulations and autologous FG from human donors, or the influence of fibrin concentration and reaction times on the adhesion strength onto

D. Trucco, L. Riacci, L. Vannozzi, L. Arrico, L. Ricotti
The BioRobotics Institute
Scuola Superiore Sant'Anna
Piazza Martiri della Libertà 33, Pisa 56127, Italy
E-mail: diego.trucco@santannapisa.it

D. Trucco, L. Riacci, L. Vannozzi, L. Arrico, L. Ricotti
Department of Excellence in Robotics & AI
Scuola Superiore Sant'Anna
Piazza Martiri della Libertà 33, Pisa 56127, Italy

D. Trucco, C. Manferdini, E. Gabusi, G. Lisignoli
IRCCS Istituto Ortopedico Rizzoli
SC Laboratorio di Immunoreumatologia e Rigenerazione Tissutale
Via di Barbiano, 1/10, Bologna 40136, Italy

 The ORCID identification number(s) for the author(s) of this article can be found under <https://doi.org/10.1002/mabi.202200096>

© 2022 The Authors. Macromolecular Bioscience published by Wiley-VCH GmbH. This is an open access article under the terms of the Creative Commons Attribution License, which permits use, distribution and reproduction in any medium, provided the original work is properly cited.

DOI: 10.1002/mabi.202200096

the skin^[14]). In particular, Dehne et al. have analyzed the bonding strength of FG-based tissue adhesives on bone and cartilage tissues, testing different timings (30 and 60 s) between FG delivery and the subsequent adhesion of bone/cartilage samples or a poly(lactic-co-glycolic acid) scaffold.^[15] The authors found that the adhesive strength was higher for 60 s with respect to 30 s. However, no hints are still available on FG efficiency as a primer for a broader range of time points (over 60 s), and on hydrogels to be crosslinked in situ on the cartilage site.

CNFs at a concentration of 0.5% (w/v) have been recently proposed as a solution to increase the adhesion strength of poly(ethylene glycol) dimethacrylate/alginate (PEGDMA) hydrogels to the articular cartilage.^[16] The physical entrapment of CNFs within hydrogels was ensured by the formation of hydrogen bonds due to their hydrophilic nature and CNFs acted as mechanical interlocks to integrate materials with tissues.^[17] They also represented a biocompatible reinforcement that improved the hydrogel mechanical properties.^[18,19] However, no insights are reported in the state-of-the-art on the behavior of CNFs-embedded hydrogels acting as an adhesion promoter layer using different concentrations of CNFs.

CATs constitute another interesting strategy for promoting material adhesion to surfaces. In a recent study, CAT-modified gelatin synthesized via an EDC/NHS (1-ethyl-3-(3-dimethyl aminopropyl) carbodiimide/*N*-hydroxy succinimide) chemistry has been employed as a light-triggered primer, reporting low cytotoxicity^[20] and good adhesive behavior. However, no comparisons between CATs, FG and CNFs-embedded hydrogels used as primers are available in the state-of-the-art.

In recent years, gellan gum (GG) has been widely studied for cartilage tissue engineering due to its biocompatibility, biodegradability, and ductility.^[21–25] GG is a water-soluble anionic polysaccharide produced by the bacterium *Sphingomonas elodea*. Its structural similarity with native articular cartilage glycosaminoglycans due to the presence of glucuronic acid residues in its repeating unit makes it attractive for cartilage-related applications. Moreover, this polymer has shear-thinning properties and allows gel formation at body temperature, characteristics that favor its use as an injectable material. In this paper, we report the systematic comparison of adhesion strength between FG, CNFs and CATs used to GG. The investigation was carried out on GG hydrogels crosslinked both ionically (using $MgCl_2$,^[21]) or using visible light (by methacrylating the GG, thus turning it into a photocrosslinkable polymer).

2. Results and Discussion

As shown in **Figure 1a**, FT-IR spectra of GG and GGMA both presented the typical gellan gum IR bands at 3300 cm^{-1} (O–H stretching), 2900 cm^{-1} (C–H stretching), 1604 cm^{-1} (COO asymmetric stretching), 1404 cm^{-1} (COO symmetric stretching), and 1020 cm^{-1} (C–O stretching), in agreement with previous literature reports.^[22–26] In the case of GGMA, an additional band characteristic of the methacrylic group at 1708 cm^{-1} appeared (C=O stretching), confirming the modification of the native GG.^[23,26]

Further verification of the GG modification was carried out by recording the ^1H NMR spectrum (**Figure 1b**). Both the NMR spectra showed the typical resonance peak of the rhamnose methyl group at 1.45 ppm. However, in the case of GGMA, a set of

new peaks become evident in the region 6.6–6 ppm and 2.1 ppm, associated with the protons of the methacrylic unit.^[23,26] By comparing the integrated area of the peak associated with the methyl protons of the methacrylic group (A_{MA}) and the integrated area of the rhamnose methyl unit (A_R) in the GGMA ^1H spectra, it was possible to determine the degree of methacrylation (DOM) of the GGMA, defined as follows (Equation 1)

$$\text{DOM} = \frac{A_{MA}/A_R}{n_{OH}} \times 100 \quad (1)$$

where n_{OH} is the number of reactive hydroxyl groups per repetitive unit of the native GG. In our case, the methacrylation reaction gave a GGMA with a DOM of 10%.

The swelling kinetics of the GG and GGMA hydrogels were evaluated by immersing the cross-linked gels in deionized water at $37\text{ }^\circ\text{C}$ and by evaluating their swelling ratios at specific time points (**Figure 1c**). The submersion of GG cross-linked hydrogels caused an initial decrease of the hydrogel weights, probably either as a consequence of ions exchange between the hydrogels and the water or a partial dissolution of not crosslinked polymer chains. After 1 h, the GG hydrogels reached the maximum weight loss ($-9 \pm 3\%$). Then, a slight increase of the hydrogel weight was evident up to 2 h, when it reached a value of $-4 \pm 2\%$. On the contrary, GGMA cross-linked hydrogels showed an increase in their swelling ratio. In particular, after 1 h, the swelling ratio reached a value of $74 \pm 15\%$, and remained almost constant after 2 h ($77 \pm 25\%$). This behavior points to a lower crosslinking efficiency in the case of GGMA hydrogels.

Initially, GG and GGMA hydrogels were tested to evaluate their adhesion strength without primers. As shown in **Figure 2a**, we found that the peak adhesion strength values were significantly different between GG ($2.53 \pm 0.69\text{ kPa}$) and GGMA ($6.46 \pm 1.81\text{ kPa}$) ($* p < 0.05$). Furthermore, both crosslinked hydrogels detached from the bovine cartilage samples while remaining completely intact after the tests, suggesting that the tissue and the hydrogel interface underwent rupture (**Figure S1**, Supporting Information). It has been shown that the clinical value considered suitable to permit a stable hydrogel adhesion with the surrounding tissue is at least 10 kPa .^[9] Indeed, Learmonth et al. found a rather limited adhesiveness of GG to biological tissues and a consequent scarce stability of GG-based implants.^[27] On the other hand, the adhesiveness of GGMA photocrosslinked with a visible light-sensitive photoinitiator has never been tested so far. Our results indicate that the photocrosslinked hydrogel shows a stronger adhesion than the ionically crosslinked one. A higher adhesiveness enabled by photoresponsive materials has been described for phenol- and catechol-modified gelatins tested after photo- or ionic-crosslinking,^[20] although using a slightly different set-up for the evaluation. Probably this behavior is due because ionic crosslinking typically occurs through reversible interactions, whereas photocrosslinking forms covalent bonds that increase the interface stability. A similar explanation could also be applied in the case of GG and GGMA.

The adhesion strength of GG improved in the presence of the FG primer (**Figure 2a**) with respect to the control with no primer. In particular, the maximum adhesion strength increased to $6.50 \pm 2.36\text{ kPa}$ ($** p < 0.01$), to $7.91 \pm 2.39\text{ kPa}$ ($** p < 0.01$) and 12.64

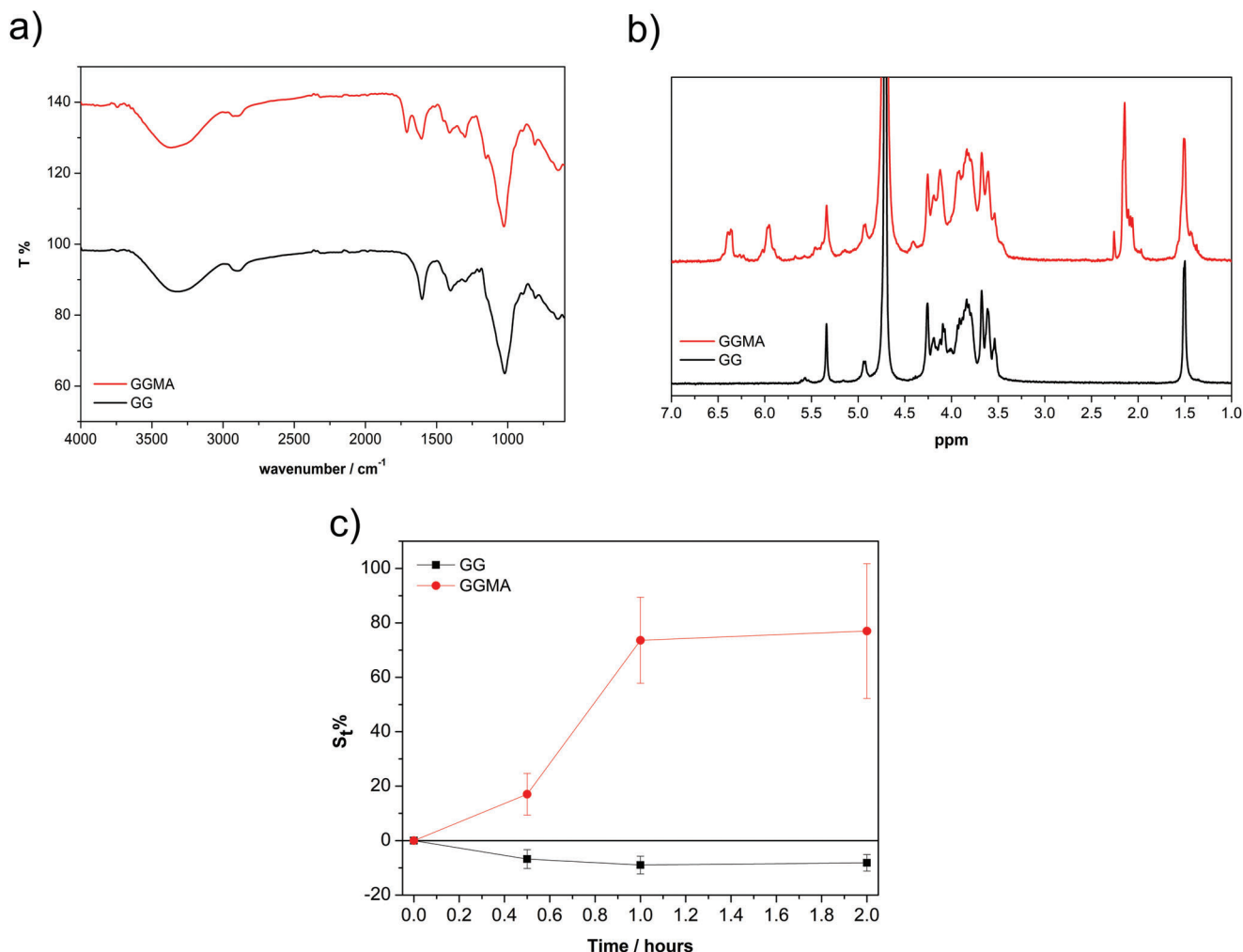


Figure 1. a) ATR FT-IR spectra of the native GG (black) and GGMA (red). b) ¹H NMR spectra of GGMA (red) and GG (black). c) Swelling ratio of GG (black) and GGMA (red) hydrogels in deionized water measured at 30 min, 1, 2, 5, and 24 h. In the case of GGMA hydrogels, the measurements were carried out only for 2 h.

± 0.87 kPa (** $p < 0.01$) after 30 s, 5 min and 15 min, respectively, while it decreased to 4.64 ± 0.99 kPa after 30 min with a statistically significant difference with respect to the 15 min value (** $p < 0.01$).

Analyzing the adhesion strength of GGMA (Figure 2a), we found no statistically significant differences among the tested conditions. Nonetheless, the maximum adhesion strength trend tended to slightly increase with respect to the control (no primer) in the sample provided with FG. The strength values resulted 7.58 ± 0.91 kPa (after 30 s), 9.80 ± 3.03 kPa (after 5 min), 10.99 ± 3.14 kPa (after 15 min) and 7.71 ± 2.01 (after 30 min) (Figure 2a). Only the waiting time of 5 and 15 min guaranteed clinically acceptable values (≈ 10 kPa), on average. Although the adhesion strength values did not differ considerably between GG and GGMA hydrogels provided with a FG adhesion layer, the stress-strain curves instead had a different behavior.

Analyzing average stress-displacement curves for GG (Figure 2b), the timing of 5 min and 15 min showed a fragile behavior, with the highest peak reached before a displacement of 0.1 mm, then the stress sharply decreased to zero. Differently,

after 30 s and 30 min, the hydrogels showed a ductile behavior. For GGMA, all cases showed a clear ductile behavior, as shown in Figure 2c. The work of adhesion of GG cases did not show significant differences between the samples (Figure 2d). We observed a statistically significant difference between GG and GGMA for samples evaluated after 5 min (* $p < 0.05$). The area calculated for the GGMA samples gradually increased reaching a maximum for the 15 min time-point, with statistically significant differences with respect to the “no primer” condition (** $p < 0.01$) and to the 30 s time-point (* $p < 0.05$). Then, it decreased for the 30 min time-point (** $p < 0.01$), showing a similar trend as the maximum adhesion strength values. Interestingly, the work of adhesion, which derived from the strength-displacement curve, larger values were reached in the case of GGMA due to its ductile behavior. The GGMA, being a photocrosslinked matrix, resembles a less fragile and more dissipative matrix than GG.^[16]

Analyzing the interface between the tissue and the applied hydrogel more in depth, we observed that the FG always detached from the cartilage when left for only 30 seconds before GG/GGMA casting, revealing that such a time was not sufficient

Fibrin Glue

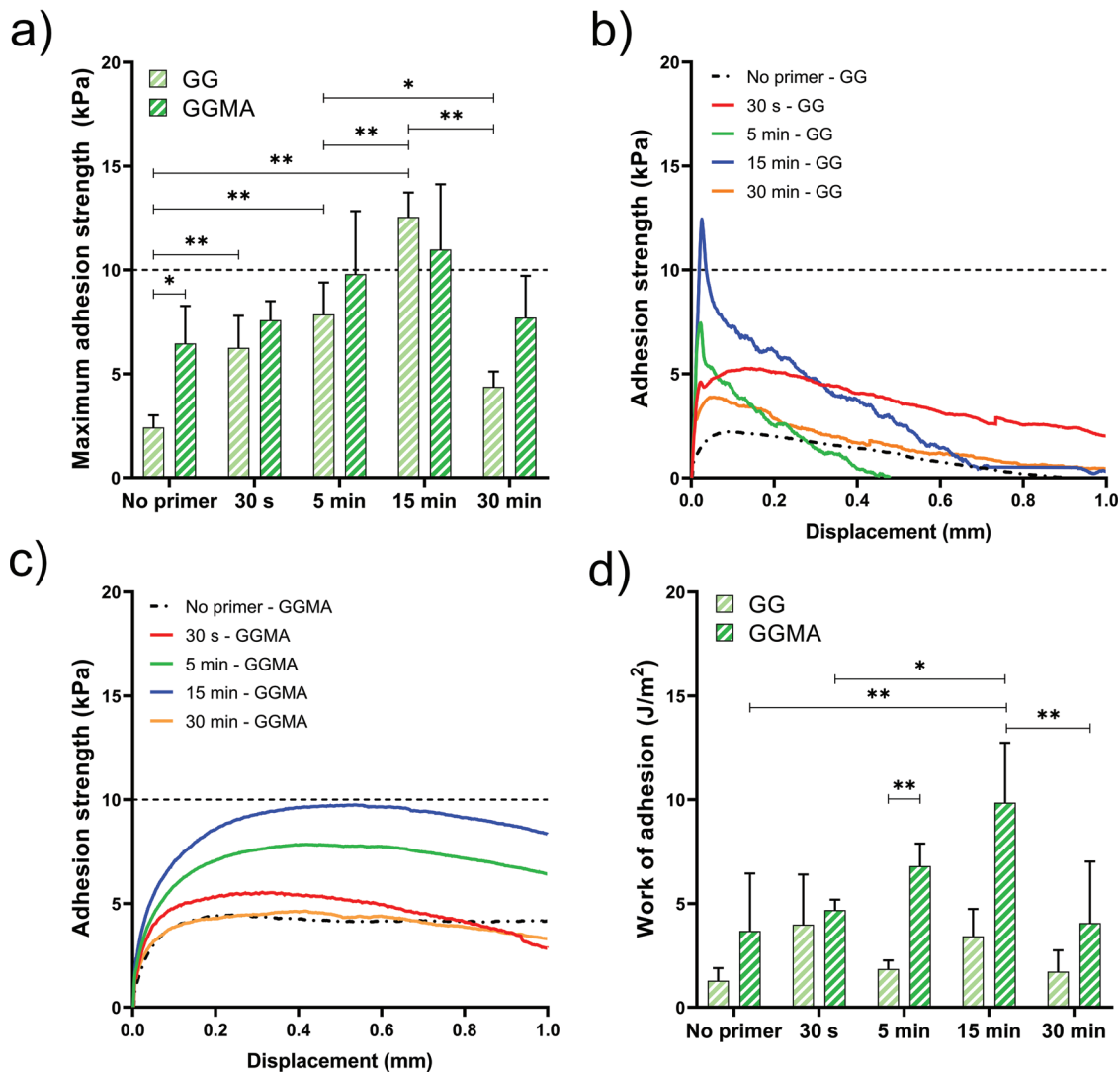


Figure 2. Adhesion test of GG and GGMA hydrogels to the cartilage using fibrin glue as a primer, evaluated at different waiting times between primer and hydrogel deposition: 30 s, 5 min, 15 min, and 30 min. a) Maximum adhesion strength values found for GG and GGMA at various waiting times for the fibrin glue. b) Adhesion strength over displacement curves for GG. c) Adhesion strength over displacement for GGMA. d) Work of adhesion of GG and GGMA calculated as the area below the adhesion strength over the displacement. The dashed line represents the adhesion strength threshold (10 kPa) suitable for clinical applications^[9]; * $p < 0.05$, ** $p < 0.01$.

for the FG to guarantee an effective adhesive behavior to the tissue (Figure S2a–d, Supporting Information). On the contrary, when the FG was left onto the cartilage to react for 5 min (Figure S2e–h, Supporting Information) and 15 min (Figure S2g–l, Supporting Information), the primer presented a higher adhesive behavior since it remained at least adhered to the cartilage sample. Interestingly, in the case with the highest adhesion strength (GGMA, 15 min), parts of the GGMA hydrogels also remained adhered, demonstrating the higher effectiveness of such a parameter setting (Figure S2k–l, Supporting Information). Lastly, the FG showed a dehydrated or vitreous-like appearance in the case of the longest time-point (30 min), as shown in Figure S2m–p (Supporting Information).

Dehne et al. evaluated two different waiting times (30 s and 60 s) for the FG, focusing on specific clinical scenarios (e.g., bone on bone, cartilage on cartilage, pull-out cartilage, and pull-out transplant).^[15] Considering the pull-out transplant model, which is the condition closest to our study, the adhesion strength resulted in 33.7 and 47.2 kPa for 30 and 60 s, respectively. These values are not comparable with the ones found in our case (due to different hydrogels tested, a different set-up used and different waiting times—we did not test 60 s), but anyhow confirmed larger values for higher time-points. Our results allowed clarifying the FG adhesive layer behavior at longer time points. The decrease of the adhesion strength when 30 min passed between FG deposition and hydrogel deposition could be due to the layer

Table 1. Sol fraction (%) of GGMA hydrogels with embedded CNFs at a concentration of 0.1% w/v and 0.5% w/v, photocrosslinked varying the exposure time: 2.5, 5, and 10 min.

Exposure time	CNFs 0.1% w/v	CNFs 0.5% w/v
2.5 min	34.74 ± 22.26	28.02 ± 3.67
5 min	14.43 ± 5.04	11.90 ± 6.73
10 min	9.15 ± 8.47	3.89 ± 1.61

drying exposed to the air and thus a lack of efficacy over time. Indeed, increasing the waiting time between the FG application and the hydrogel solution pouring, the FG may totally crosslink and also dehydrate, thus gradually losing its stickiness property toward the hydrogels. The absorption of GG and GGMA solutions within FG may occur before their crosslinking, leading to a possible FG/GG entanglement. Nonetheless, such a hypothesis seems insufficient for justifying the adhesive properties when the hydrogel solutions are applied after 30 min, as also highlighted by the results. The FG composition is an important parameter to be taken into account. Indeed, the time needed for the FG to crosslink is strongly affected by the thrombin/fibrinogen concentration, which determines the setting time of the fibrin sealant, ranging from 30 s (rapid setting) to several minutes (slow setting).^[28] The composition also affects the conversion of fibrinogen into fibrin clots, which form a mesh and an dense protofibril packing with a nanometer size, which probably impedes the entanglement of the GG polymeric chains (the average weight of the polymeric chains is 500 000 Da) upon FG assembly. This may hamper material penetration within the crosslinked solution over time.^[29] Thus, the 15 min time-point represents the best compromise, in our case, for the formation of the FG clot while the GG/GGMA remains entangled within the FG solution before its complete crosslinking.

Our results about FG are in line with those shown by Karami et al.,^[16] in which the use of another FG (from Tisseel, Baxter International Inc.) showed an adhesion strength up to 14.3 ± 2.6 kPa between the cartilage and a photocrosslinked hydrogel (in their case, a double-network matrix composed of covalently crosslinked PEGDMA and ionically crosslinked alginate reinforced with CNFs). However, in this study, the authors did not evaluate the role of the waiting time before primer and hydrogel deposition, but they rather tested the stability of the hydrogel deposited immediately after the FG deposition.

Concerning CNFs, two concentrations (0.1% and 0.5% w/v) were evaluated without testing any waiting time because the CNFs were embedded directly into the GG and GGMA hydrogels, subsequently crosslinked (with ions or light, respectively). Thus, to test these primers, such intermediate layers were produced to let the hydrogels adhere to the cartilage. First, we evaluated the crosslinking degree of GGMA hydrogels with CNFs embedded by measuring the sol fraction (%) at different time points.^[30]

Table 1 shows that the sol fraction (%) increased (average values from 9.15 to 34.74) while decreasing the exposure time to the visible light (from 10 to 2.5 min). A shorter crosslinking time may leave unreacted MA moieties in the primer layer, leading to a stronger adhesion between primer and GGMA hydrogels, poured subsequently, after the final hydrogel crosslinking of 10 min.

Following this hypothesis, we proceeded with the evaluation of the GGMA with CNFs embedded, applying an exposure time of 2.5 min for the primer crosslinking.

Regarding the adhesion test results, the CNFs improved the stress needed to detach the GG hydrogels from the cartilage with respect to the bare materials (**Figure 3a**) but resulted smaller than the ones achieved using FG (15 min) as a primer. Interestingly, the adhesion strength reached a value of 12.13 ± 4.69 kPa in the case of 0.1% w/v CNFs (statistically higher than the no primer condition), while the strength was smaller for a higher concentration of fibers (0.5% w/v), reaching a value of 6.56 ± 2.58 kPa, still higher with respect to the control, but without a significant statistical difference. Thus, only the smaller concentration of CNFs (0.1% w/v) allowed overcoming the clinically acceptable value (10 kPa). Similarly to GG, GGMA also showed higher adhesion when a CNF concentration of 0.1% w/v was used as a primer (9.71 ± 3.84 kPa), with respect to the absence of primer (**Figure 3a**) but without statistically significant differences. Also in this case, a slight decrease was observed when 0.5% w/v CNFs was applied respect to 0.1% w/v sample, resulting in an adhesion strength of 6.91 ± 3.58 kPa. From such results, the higher concentration of CNFs seemed to be detrimental to our purpose.

The interface constituted by the embedding of CNFs at a concentration of 0.1% w/v endowed the GG with a ductile behavior, as shown in **Figure 3b**, while the case of 0.5% w/v a fragile behavior was found. Also in the case of GGMA, the use of CNFs at 0.1% w/v provided a slightly ductile-like behavior, despite the presence of an initial peak before the displacement of 0.1 mm, while a fragile behavior was found for the 0.5% w/v concentration (**Figure 3c**).

The corresponding areas under the curve were considerably higher in the case of 0.1% w/v CNFs, with respect to the absence of primer (***p* < 0.01) for GG and GGMA (**Figure 3d**). Also for this primer, the cases with a ductile-like behavior showed a higher performance in terms of maximum adhesion strengths, in agreement with Karami et al.^[16]

Analyzing the interface between the tissue and the hydrogels, we noticed that the primer layer remained intact on the bovine cartilage sample after the adhesion tests for both GG and GGMA, suggesting that the interface between the primer and the hydrogel underwent rupture (**Figure S3**, Supporting Information).

To the best of our knowledge, this is the first time that a ionically crosslinked hydrogel is tested in terms of adhesion strength using CNFs. The mechanism through which CNFs act is probably similar to the one reported by Karami et al.^[16] The authors showed that the ability of the hydrogels to transfer energy was improved due to entanglement effects allowing to generate hydrogen bonds and thus increasing the overall bonding energy, as well as the density of contact points between the tissue surface and the hydrogel (enabled by nanoscale fibers), resulting in an enhancement of the interface quality.^[16] Karami et al. assessed this behavior for a concentration of CNFs of 0.5% w/v. Our results show that this mechanism is more efficient (at least for GG and GGMA hydrogels) at a concentration of 0.1% w/v, while a higher presence of CNFs probably causes the embrittlement of the primer–tissue interface, or the primer–hydrogel one, making crack propagation upon mechanical stress more likely.

Figure 4 shows the adhesion strength results obtained with the photocrosslinked CAT-based gelatin used as the adhesive layer.

Cellulose nanofibers

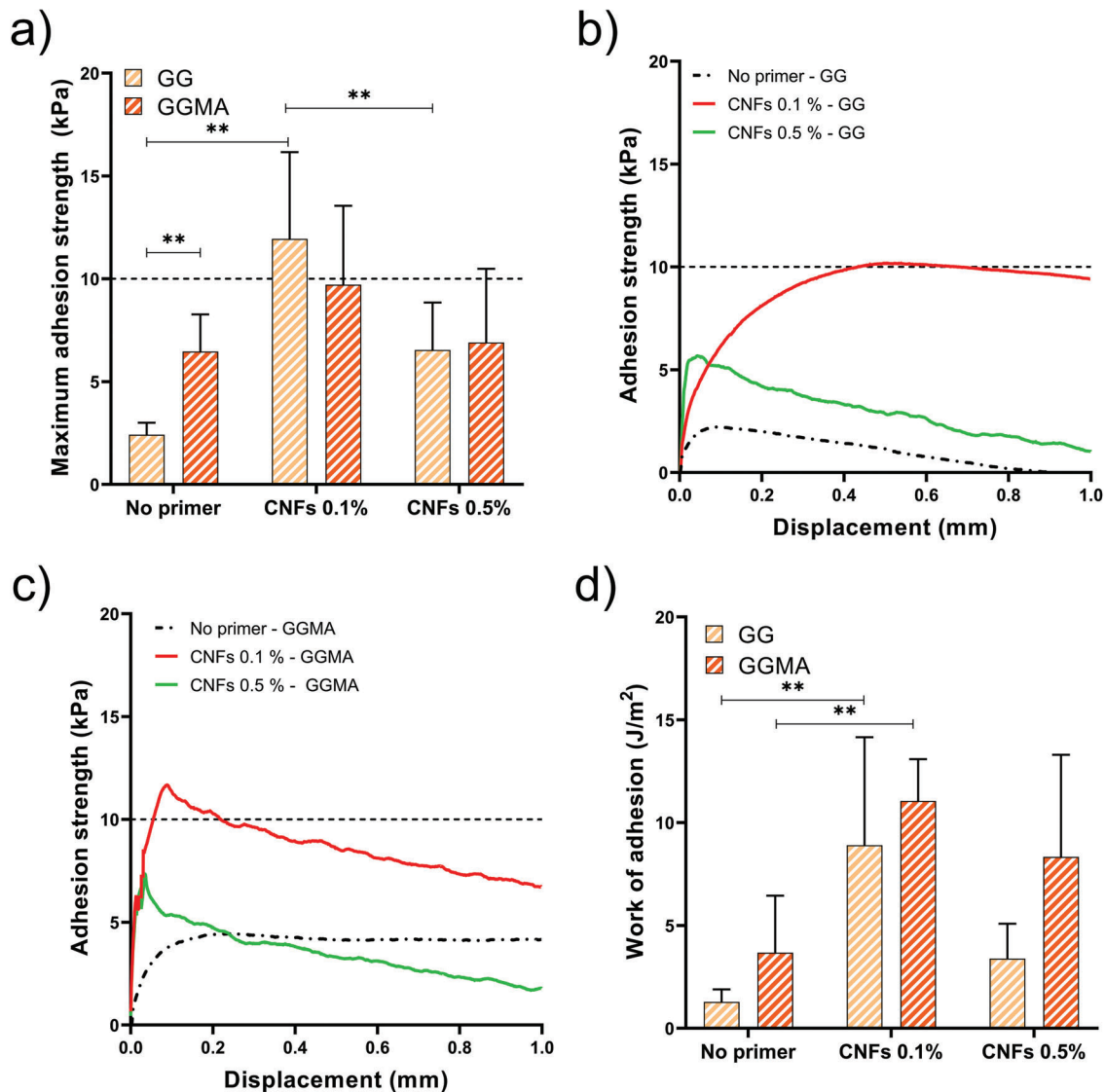


Figure 3. Data on GG and GGMA hydrogels using embedded cellulose nanofiber into a primer's layer at different concentrations: 0.1% and 0.5% w/v. a) Maximum adhesion strength values found for GG and GGMA varying the concentration of cellulose nanofibers (0.1% and 0.5% w/v). b) Adhesion strength over displacement curves for GG. c) Adhesion strength over displacement curves for GGMA. d) Work of adhesion of both GG and GGMA obtained from the adhesion test curves. The dashed line represents the adhesion clinical value equal to 10 kPa^[9]; * $p < 0.05$, ** $p < 0.01$.

For GG-based hydrogels, the adhesion strength of hydrogels deposited on the primer with CATs concentration of 100 mg mL⁻¹ slightly increased (6.16 ± 1.86 kPa) with respect to the control (** $p < 0.01$). Instead, the hydrogels deposited on the primer with 125 mg mL⁻¹ of CATs showed a strength of 8.85 ± 2.40 kPa, which resulted statistically different with respect to the control (** $p < 0.01$) and to the concentration of 100 mg mL⁻¹ (* $p < 0.05$) (Figure 4a). Regarding the GGMA, the adhesive layers at different concentrations of CATs have different effects on the stability of GGMA hydrogels on the cartilage tissue: the adhesion strength was 6.33 ± 0.74 and 8.06 ± 1.38 kPa using a CATs concentration of 100 and 125 mg mL⁻¹, respectively, showing no statistical differences between them. It was noticeable that the CAT-

based primer improved significantly only the adhesion strength of the GG-based hydrogels, ionically crosslinked. As shown in Figure 4b, CATs concentrations of 100 and 125 mg mL⁻¹ showed a fragile behavior with GG. Such behavior was similar for the GGMA case applied after the CATs at 125 mg mL⁻¹, while in the case of 100 mg mL⁻¹ the hydrogels showed a more ductile behavior, similar to the no primer condition (Figure 4c).

A relatively small work of adhesion for GG was found in both cases when compared with the previously analyzed primers, as shown in Figure 4d, finding a significant difference between the condition without primer and the condition at 125 mg mL⁻¹. For GGMA, as shown in Figure 4d, the work of adhesion values resulted similar to the GG cases with no significant differences.

Catecholamines

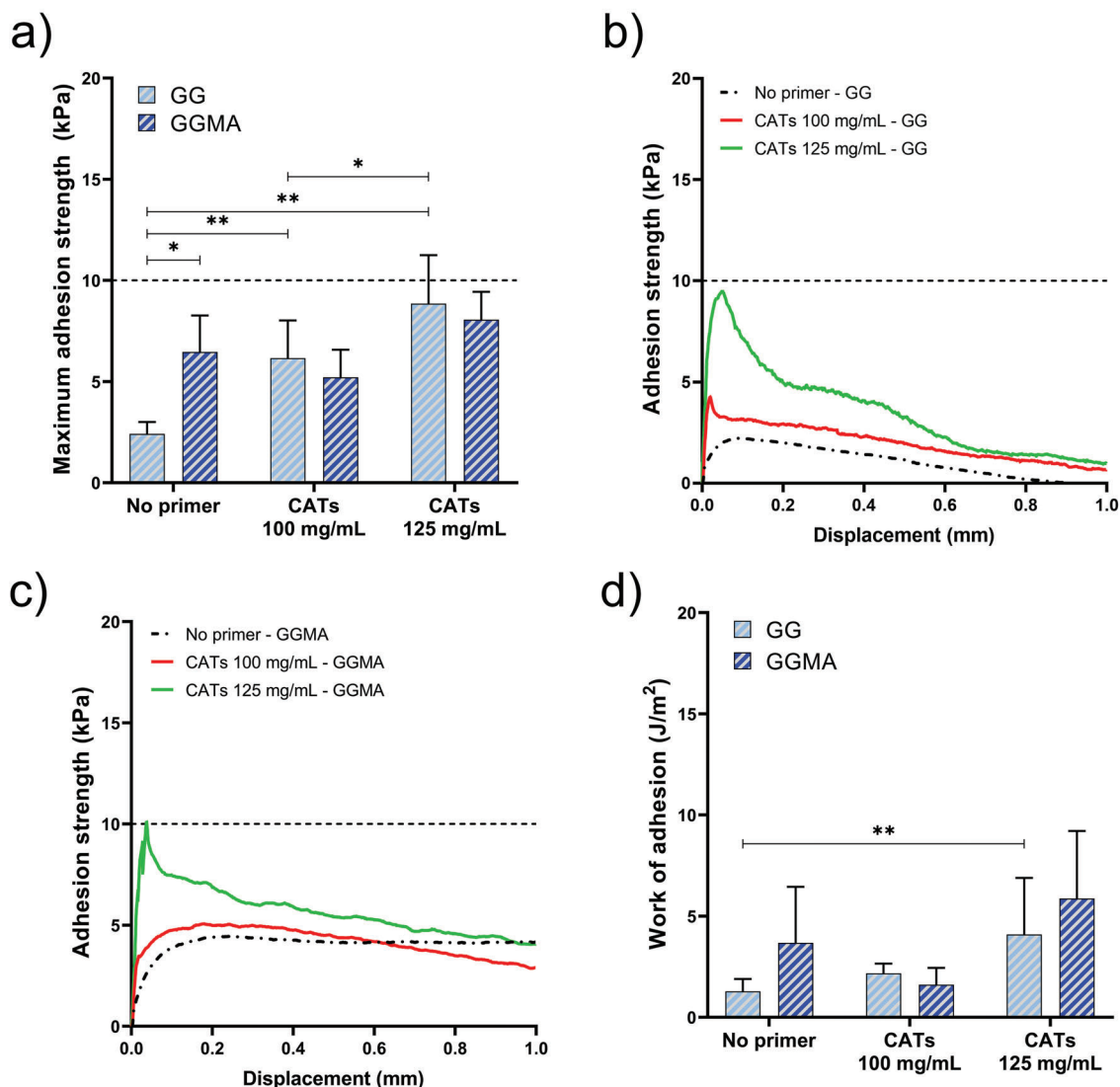


Figure 4. Data on GG and GGMA hydrogels using a photocrosslinked catecholamines-based layer at two different concentrations between the bovine cartilage sample and the hydrogel: 100 and 125 mg mL⁻¹. a) Maximum adhesion strength values found for GG and GGMA varying the catecholamines concentration. b) Adhesion strength over displacement for GG. c) Adhesion strength over displacement for GGMA. d) Work of adhesion obtained from the adhesion test curves for both GG and GGMA. The dashed line represents the adhesion clinical value equal to 10 kPa^[9]; * $p < 0.05$, ** $p < 0.01$.

The low energy of absorption due to the fragile behaviors reflected a low performance of CAT-based primers for both GG and GGMA hydrogels, in agreement with.^[16]

Our data do not match with the values found by Liu et al. (61.8 ± 1.8 kPa in the presence of a CAT-based primer).^[20] However, in this study the authors evaluated the role of CAT layers by testing the adhesion between two egg membranes, thus not employing a cartilage tissue and a specific hydrogel, and using a different tensile set-up, thus making their results and ours poorly comparable. As shown in Figure S4 (Supporting Information), the interface provided by the CAT-based primer at both concentrations remain adhered to the bovine cartilage tissue after the adhesion test. In all cases, the hydrogels detached from the primers.

By comparing all data, we evidenced that the highest adhesion strength was obtained using the FG and injecting the hydrogel solutions after 15 min (12.64 ± 0.87 kPa for GG and 10.99 ± 3.14 kPa for GGMA) (Figure 2a). In view of the results obtained with this analysis, we further tested such an optimal adhesive condition by embedding 10^6 cells mL⁻¹ within each hydrogel type, thus simulating another potential clinical scenario (injection of a cell-laden hydrogel on the cartilage site). As shown in Figure 5a, the maximum adhesion strength of GG significantly decreased from 12.64 ± 0.87 kPa (without cells) to 9.52 ± 1.10 kPa (with embedded cells) (** $p < 0.01$).

The GGMA also showed a decrease from 10.99 ± 3.13 kPa to 9.27 ± 0.68 kPa, although the difference was not significant (Fig-

Cell-embedded GG/GGMA using fibrin glue primer (15 min)

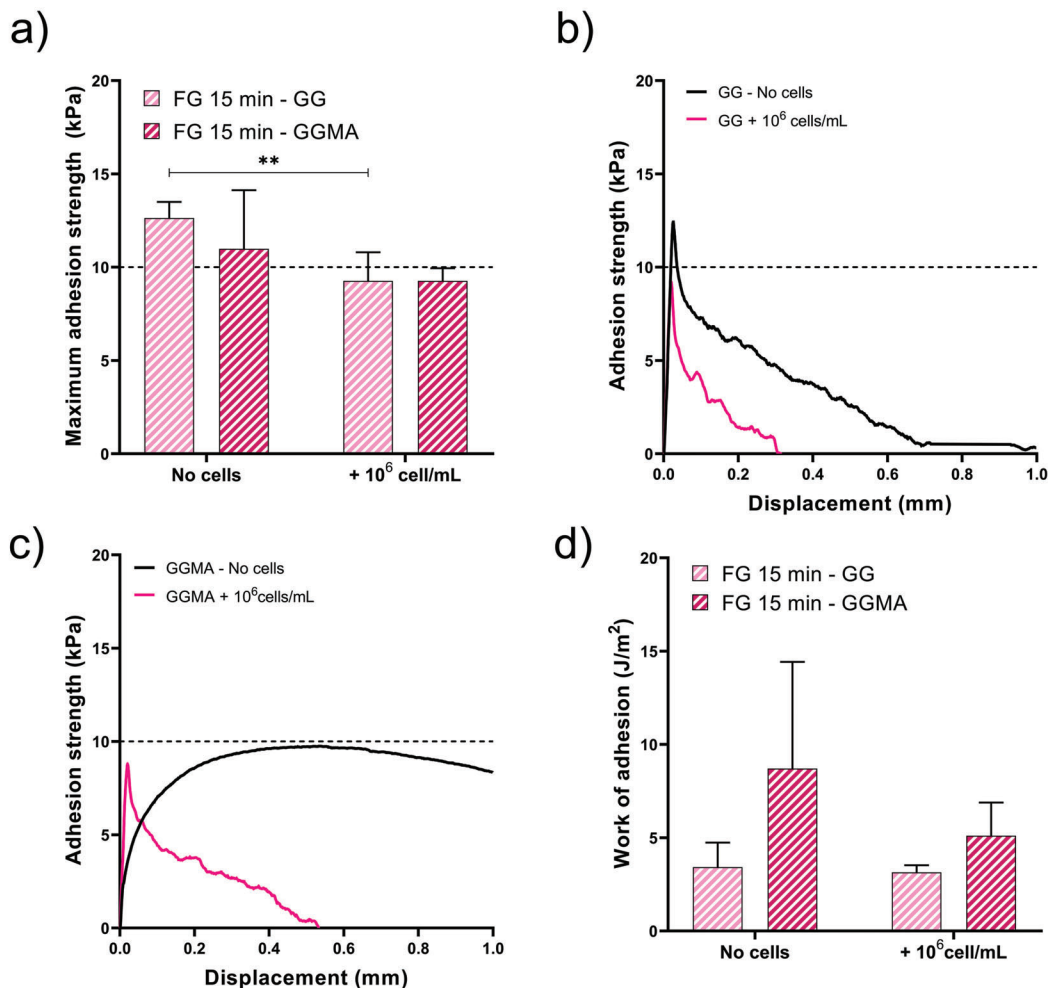


Figure 5. Data on GG and GGMA hydrogels using fibrin glue 15 min (the best condition from previous evaluations) and comparing cases without and with embedding 10^6 cell mL^{-1} . a) Maximum adhesion strength values found for GG and GGMA for the best fibrin glue condition, with and without cells. b) Adhesion strength over displacement for GG. c) Adhesion strength over displacement for GGMA; d) Work of adhesion of both GG and GGMA obtained from the adhesion test curves. The dashed line represents the adhesion clinical value equal to $10 \text{ kPa}^{[9]}$; In all graphs, data about fibrin glue 15 min without cells was compared with data about fibrin glue 15 min with embedded cells. $** p < 0.01$.

ure 5a). A fracture behavior was found in both cases (Figure 5b,c), similar to the “no cells” condition for the GG, and slightly different for the GGMA hydrogel, which behavior was more ductile for the cell-free formulation. Despite the decrement in adhesion strength caused by the presence of cells, such a condition still showed a performance that is in line with the clinically acceptable threshold of 10 kPa . To get more insights on the crosslinking degree of the GGMA hydrogels, we evaluated the GGMA sol fraction without and with embedding cells. Results demonstrated the absence of a statistically significant difference, being the sol fraction $7.49 \pm 3.01\%$ (without cells) and $6.51 \pm 1.31\%$ (with cells), respectively.

Finally, the work of adhesion (Figure 5d) of both hydrogels resulted similar (without any statistical difference) in the presence and absence of cells. However, in GGMA, the work of adhesion of cell-laden hydrogel was lower with respect to the “no cell” condition, even if not statistically relevant.

With respect to the existing state-of-the-art, this is the first time that the adhesion strength of GG-based hydrogels with embedded cells onto cartilage tissues is reported in the presence and the absence of an adhesive primer. Despite the extensive literature existing on chemical and photoreactive tissue adhesives, our outcomes show the possibility to make bare hydrogels (GG and GGMA) adhesive to the cartilage without chemically modifying them with tissue adhesive cues.^[31]

2.1. Biological Evaluations on hASCs Laden in GG and GGMA Hydrogels

Live/Dead staining showed a high number of viable cells (shown in green) in both hydrogels on days 2 and 7 after seeding (Figure 6a). Conversely, a low number of dead cells (shown in red) was found in all hydrogels.

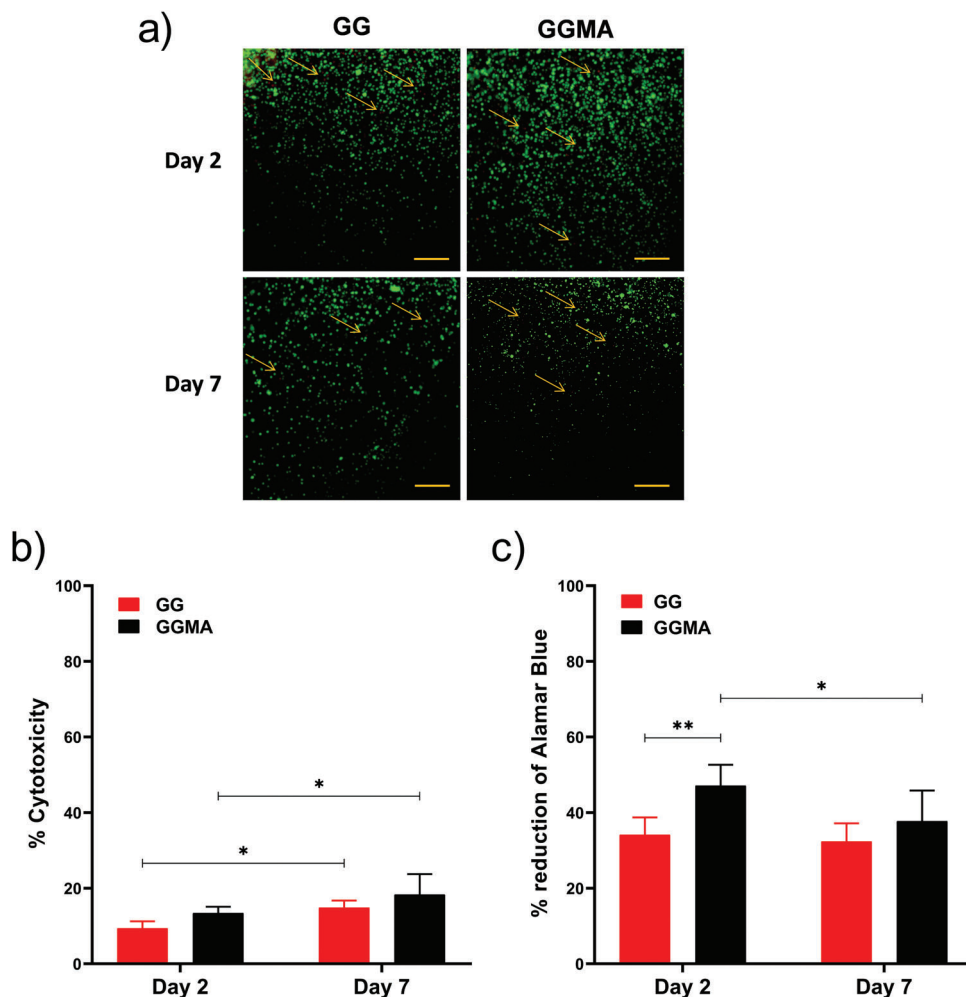


Figure 6. a) Live/Dead assay performed on hASCs encapsulated in GG and GGMA hydrogels on day 2 and 7. Viable cells are shown in green; dead cells are red (indicated by yellow arrows). Scale bars = 100 μm . b) LDH release from hASCs embedded in GG and GGMA hydrogels on day 2 and 7. Data are expressed as a percentage of cytotoxicity. c) AlamarBlue analysis of hASCs embedded in GG and GGMA hydrogels on day 2 and 7. Data are expressed as a percentage of the reduction of AlamarBlue. Data presented as mean \pm SD, $n = 5$; * $p < 0.05$, ** $p < 0.01$.

Lactate dehydrogenase (LDH) release was assessed to evaluate the hydrogel cytotoxicity on hASCs. Although the detected enzyme slightly increased on day 7 in both hydrogels, its level remained lower or equal to 20% in all hydrogels analyzed (Figure 6b). Both formulations confirmed that the microenvironment created by the hydrogels did not negatively affect the encapsulated hASCs, supporting the nontoxic nature of the hydrogel matrices following the UNI EN ISO 10993–5:2009.

Moreover, the analysis of metabolic activity showed that on day 2 the amount of metabolically active cells in the GGMA hydrogels was statistically significant higher respect to the GG ones but remained similar on day 7 (Figure 6c). A slight but statistically significant decrease (* $p < 0.05$) of the metabolic activity was observed for GGMA between day 2 and day 7. However, cell viability can be considered high in all formulations.

Finally, we analyzed hASCs migration both toward and outward the hydrogels. As shown in Figure 7a–c, we observed a higher cell migration toward the GGMA compared to the GG hydrogels (Figure 7b). Similarly, the migration of hASCs from

inside to outside of hydrogels was significantly higher in the GGMA with respect to the GG (Figure 7c).

In this work, for the first time, the cell migration properties of GG-based hydrogels were evaluated. As reported in Bacelar et al.,^[32] GG hydrogels lack anchorage points for cell adhesion (i.e., Arg-Gly-Asp peptide); the absence of cell-adhesive cues has been attributed to their extreme hydrophilic nature. However, our results highlight that GGMA guarantees a better cell migration than GG. This could be due to the presence of hydrophobic methacrylic groups in GGMA, changing the hydrogel capability to bind water molecules to the polymer backbone and, consequently, positively affecting cell migration^[23].

3. Conclusion

A stable adhesion to the target tissue is of paramount importance for the clinical translation of hydrogels in the orthopedic field. A systematic comparison between fibrin glue, cellulose nanofibers and catecholamines used as primers to promote the adhesion

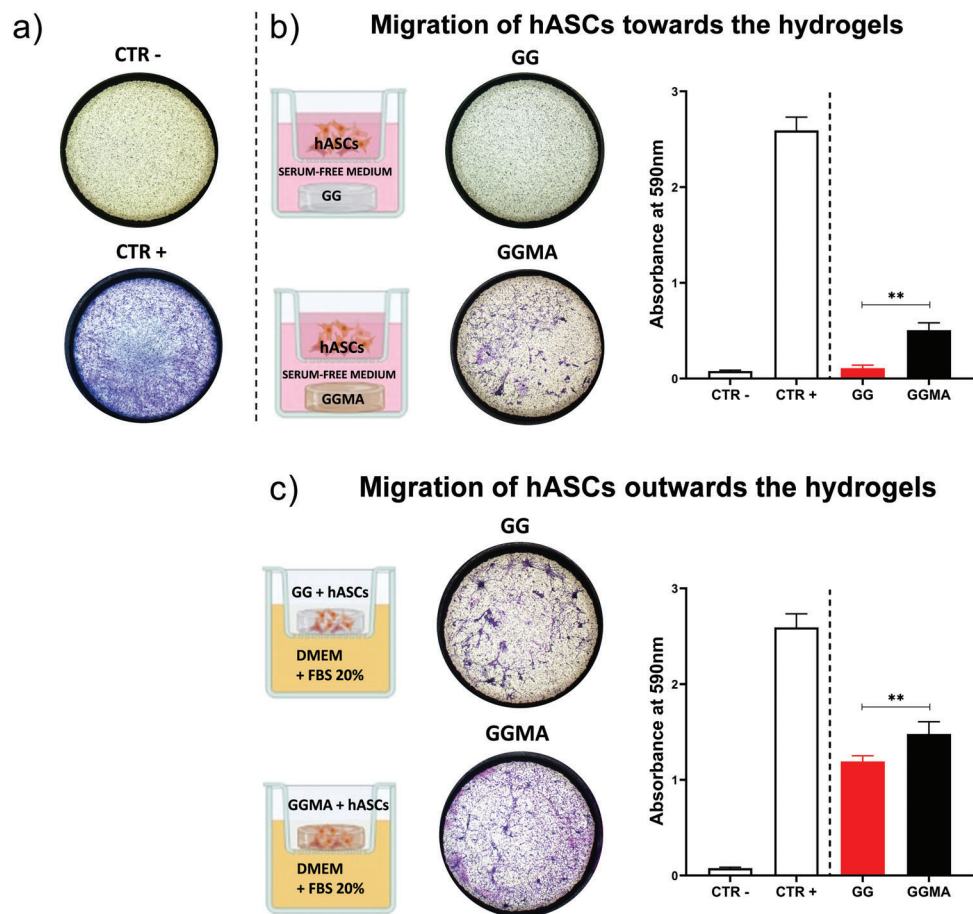


Figure 7. a) Representative images of negative and positive controls (CTR– and CTR+); b) analysis and quantification of the migration of hASCs toward the hydrogels; c) analysis and quantification of the migration of hASCs outward the hydrogels. Data presented as mean \pm SD, $n = 6$; ** $p < 0.01$.

strength of polysaccharide-based hydrogels was performed. In particular, we tested hydrogels based on gellan gum (GG) and its methacrylated derivative GGMA. GGMA was obtained starting from the pristine GG through a methacrylation procedure that allowed us to introduce methacrylic units onto the backbone of GG and to achieve a degree of methacrylation of $\approx 10\%$, as observed by FT-IR spectroscopy and quantified by ^1H NMR analysis. Ionically crosslinked GG and photocrosslinked GGMA hydrogels showed different swelling behaviors, indicating a higher crosslinking efficiency in the case of the GG-based hydrogel. In addition, the investigation of the adhesion strength on ex vivo cartilage tissue revealed that photocrosslinked GGMA showed a higher adhesion strength with respect to ionically crosslinked GG hydrogels in the absence of primers. However, in both cases, the adhesion strength values found were far from clinically acceptable ones. With the fibrin glue applied as a primer, the best condition for both hydrogel types resulted in a waiting time of 15 min between primer deposition on the cartilage and subsequent hydrogel pouring. The embodiment of cellulose nanofibers within GG and methacrylated GG increased the adhesion strength of both hydrogels for a fiber concentration of 0.1% w/v, while the use of a higher concentration (0.5% w/v) was detrimental. A CAT-modified gelatin layer used as a primer was not effective

to promote the adhesion between the GG-based hydrogels and the cartilage. The condition showing the best performance (fibrin glue and a waiting time of 15 min before hydrogel pouring) was also evaluated after embedding hASCs into the hydrogels, thus to mimic a possible translation-relevant scenario in the regenerative medicine field. Results showed a slight decrease in the adhesion strength for the cell-laden hydrogel with respect to the cell-free one, for both GG-based hydrogels, but still compatible with the clinically acceptable threshold. Biological experiments on GG and GGMA hydrogels embedding hASCs showed that both GG-based hydrogels are able to host viable cells at least for 7 days, and both hydrogels permit hASCs migration. Interestingly, GGMA considerably favored cell migration toward and outward the hydrogel, with respect to GG.

The results of this study highlight the potential of using primers as intermediate layers to improve the adhesion of injectable materials to be crosslinked in situ, without the need for chemical modifications of the hydrogel. These results can be relevant for future in vivo translation of injectable hydrogels for substituting or regenerating chondral and osteo-chondral tissues, although further efforts should be conducted in the future to assess if the adsorption of proteins and other molecules found in the vivo scenario could interfere with the priming process.

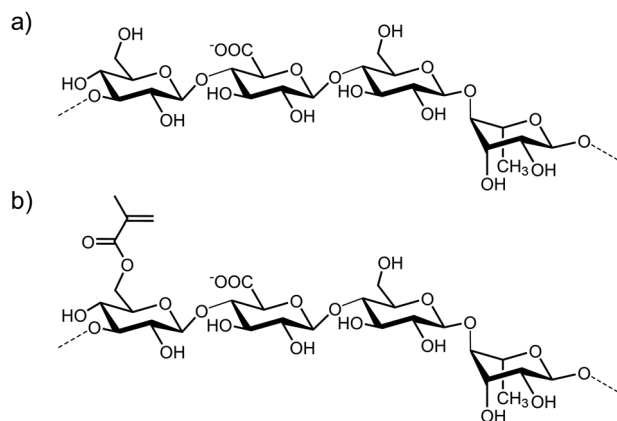


Figure 8. Chemical structure a) of the repetitive units of GG and b) of a representative repetitive unit of GGMA.

4. Experimental Section

Materials Preparation and Chemical Characterization: Gellan gum (GG) was purchased from Merck (trademarked as Gelzan CM by CP Kelco, USA). GG is a linear polymer where the repeating unit is $[\rightarrow 3\text{-}\beta\text{-D-glucose-(1}\rightarrow 4\text{)-}\beta\text{-D-glucuronic acid-(1}\rightarrow 4\text{)-}\alpha\text{-L-rhamnose-(1}\rightarrow)]$, as detailed in **Figure 8a**. The molecular weight of GG was 10^6 Da, as reported in the certificate of analysis of the used Gelzan CM (lot # SLCH0978).

To obtain the methacrylated gellan gum (GGMA, **Figure 8b**), a methacrylation procedure was performed similarly to Coutinho et al.^[26] Briefly, GG was dissolved in deionized water (1% w/v) with a magnetic stirrer at 75 °C for 1 h. The solution was then cooled to 60 °C, and 8.5 mL of methacrylic anhydride (MA, Merck) per 100 mL of solution were slowly added. The solution reacted for 6 h at a controlled pH range (8–9.5), then was centrifuged (3500 rpm for 3 min) at 30 °C to remove the unreacted MA, and the supernatant was diluted (1:2) with deionized water pre-heated at 40 °C. The solution was dialyzed (MWCO 12–14 kDa, Cellu Sep, USA) at 60 °C for 5 d, quickly frozen in liquid nitrogen and stored at –80 °C. Finally, aliquots were lyophilized (Labconco, FreeZone 2.5 Plus) for 3 days to obtain the GGMA powder and kept at –80 °C before use.

FT-IR spectra were collected in attenuated total reflection (ATR) mode on dry GG and GGMA powders, using an IRAffinity-1 FT-IR spectrophotometer equipped with an ATR MIRacle-10 accessory (Shimadzu Scientific Instrument, Japan). The spectra were recorded in the range 4000–600 cm^{-1} using 64 scans and a resolution of 4 cm^{-1} and they were corrected by subtracting the background spectrum recorded immediately before the samples and obtained with the same instrumental parameters. The ^1H NMR spectra were recorded on a Bruker Ascend 400 at 50 °C, using solutions of 5 mg of GG or GGMA in 1 mL of D_2O .

Fibrin glue (FG) was purchased from Ethicon (Evicel Fibrin Sealant (Human) kit): it is based on two components: a human conjugable protein (50–90 mg mL^{-1}), made mainly of fibrinogen and fibronectin, and human thrombin (800–1200 UI mL^{-1}). The two components were stored at –20 °C until use.

Cellulose nanofibers (CNFs) were purchased from Valida Visco-S (fibrillated cellulose in water, solid content: $8.0 \pm 0.02\%$) as a water dispersion. To obtain the CNFs containing GG and GGMA based primers, CNFs were stirred for 2 min and then added to GG and GGMA hydrogels (2% w/v) at two concentrations (0.1 and 0.5% w/v).

CAT-modified gelatin was prepared via chemical reaction using EDC (Merck) and NHS (Merck), referring to the existing literature.^[20] The used gelatin was purchased from Merck (from porcine skin, gel strength 300, Type A). Briefly, 1.0 g of gelatin was dissolved in 100 mL of degassed 2-(N-Morpholino) ethane sulfonic acid hydrate (MES, Merck) buffer (pH 4.5, 100×10^{-3} M) at 37 °C. EDC (575.1 mg) and NHS (345.3 mg) were added to the solution. After stirring for 20 min, dopamine hydrochloride (Merck,

568.9 mg) was dissolved in 3 mL of MES buffer (pH 3.3, 100×10^{-3} M), and this solution was added to the mixture. The solution was left reacting at 37 °C in the dark and on orbital shaking at 100 rpm for 24 h. The resulting solution was purified through a dialysis membrane (MWCO 3500 Da, Cellu Sep, USA) against acidified $\text{d-H}_2\text{O}$ (pH ≈ 3) four times for 1 h and finally against deionized water (pH ≈ 7) for 2 h under vigorous stirring. The final product was lyophilized and stored at –20 °C until use.

Preparation and Characterization of GG and GGMA Hydrogels: GG hydrogel was obtained by dissolving the GG powder in deionized water at a concentration of 2% w/v by stirring for 1 h at 70 °C, and the obtained solution was kept at 37 °C for 10 min before its use. After the deposition of 400 μL of this gel, GG was crosslinked with 400 μL of MgCl_2 (Merck) solution (1% w/v in $\text{d-H}_2\text{O}$) added on the top of the hydrogel and removed after 10 min.

GGMA hydrogel was obtained by dissolving the lyophilized GGMA in phosphate-buffered saline (PBS, Merck) to achieve a concentration of 2% w/v and kept for 1 h at 37 °C. Then, tris(2,2'-bipyridyl) ruthenium(II) chloride hexahydrate (Ru, Merck) and sodium persulfate (SPS, Merck) were added to the GGMA solution at a concentration of 0.2×10^{-3} and 2×10^{-3} M, respectively, to make the solution sensitive to visible light. Ru and SPS were prepared as 20×10^{-3} and 200×10^{-3} M stock solutions in $\text{d-H}_2\text{O}$, respectively. After the deposition of 400 μL of this solution, GGMA hydrogel was crosslinked by using a white LED source (RfQ—Medizintechnik-GmbH & Co) on the top of the solution at a distance of 3 cm (intensity: 15 mW cm^{-2}) for 10 min.

For both GG and GGMA hydrogels, the swelling ratio was measured in deionized water at 37 °C. After the cross-linking procedure, the gels surfaces were gently dried with a paper tissue and their weights (w_0) were measured ($n = 5$). Then, all the gels were immersed in deionized water, and after specific time points (30 min, 1, and 2 h), they were taken out of the water, gently blotted with a paper tissue and their weights (w_t) were measured. The swelling ratio for each time point ($S_t\%$) was calculated as follows (Equation 2)

$$S_t\% = \frac{w_t - w_0}{w_0} \times 100 \quad (2)$$

Cell Cultures and Cell Encapsulation into Hydrogels: Human adipose tissue-derived stem cells (hASCs, derived from three subjects, 2 males and 1 female of 52 ± 7 years old) were purchased from Lonza (Milan, Italy). They were thawed and expanded in culture with Alpha Minimum Essential Medium ($\alpha\text{-MEM}$, Merck) containing 15% fetal bovine serum (FBS, Euroclone) and 100 U mL^{-1} penicillin/streptomycin (Life Technologies). Cells were detached from the tissue culture plate, and a concentration of 10^6 cells mL^{-1} was gently encapsulated into GG and GGMA solutions before casting and crosslinking.

Sol Fraction Analysis: The sol fraction analysis was carried out to determine the influence of the CNFs content on the crosslinking degree of the GGMA hydrogels at different light exposure doses, according to the protocol reported in Lim et al.^[30] Briefly, 200 μL of the GGMA solution were poured into a cylindrical PDMS mold (diameter = 0.8 mm, height = 0.5 mm) and then photocrosslinked as reported in the “Preparation and characterization of GG and GGMA hydrogels” section, by varying the exposure time: 10, 5, and 2.5 min.

All samples were weighed, then dehydrated through a freeze dryer (Labconco, FreeZone 2.5 Plus, Kansas City, MO, USA) and weighed again to measure their dry weight ($W_{\text{dry}1}$). At this point, PBS solution was added to all samples that were incubated at 37 °C for 24 h. Then, each sample was blotted, lyophilized and weighed ($W_{\text{dry}2}$). The sol fraction (%) was calculated as follows (Equation 3)

$$\text{Sol fraction (\%)} = \frac{W_{\text{dry}1} - W_{\text{dry}2}}{W_{\text{dry}1}} \times 100 \quad (3)$$

Set-Up and Procedure for Adhesion Strength Testing: A dedicated set-up to evaluate the adhesion strength of hydrogels to the cartilage tissue was designed on SDK Solidworks 2020. It was thought to be adapted to an

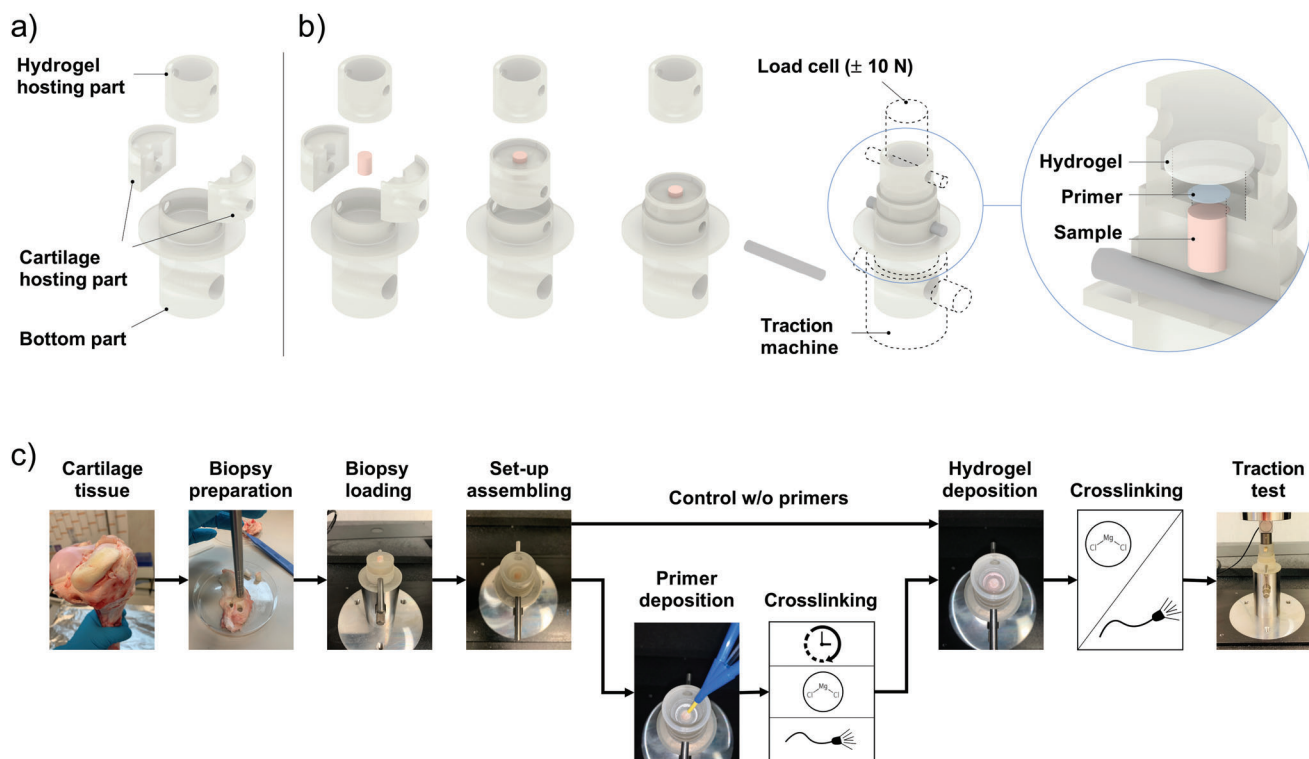


Figure 9. a) Depiction of the components of the set-up for the adhesion strength test. Single parts (bottom part, cartilage-hosting parts, and hydrogel-hosting part) are shown. b) Assembly of the set-up: the biopsy from bovine cartilage is loaded, and the set-up is assembled to block it. Finally, the set-up is fixed to the load cell (± 10 N) of the Instron Mechanical Testing System to perform the traction test. The zoomed image shows the hydrogel-hosting part cross-section to identify primer and hydrogel position on the cartilage biopsy. c) Depiction of the adhesion strength test steps: biopsy preparation from bovine cartilage, biopsy loading and set-up assembling, primer deposition (and crosslinking), hydrogel deposition, crosslinking, and adhesion strength assessment through a traction test.

Instron Mechanical Testing System (model 2444, Instron, Norwood, MA, USA) (Figure 9a). Inspired by the work of Karami et al. work,^[16] a bottom part was designed to anchor the set-up to the Instron machine through a spline. Two cartilage-hosting parts were designed to have an empty cylinder at the center (diameter = 6.4 mm; height = 7 mm) to fit in and block the cartilage tissue samples (Figure 9b). A top hydrogel-hosting part was designed to be linked to the load cell (± 10 N) of the tensile machine by using a spline and to let the pouring of the hydrogel solution directly in contact with the surface of the cartilage tissue samples on the other side. The hydrogel was poured within the hydrogel-hosting part featured by a cavity with a diameter of 15 mm and a height of 5 mm. All components were printed using a Visijet M3 Crystal material and a 3D printer (Projet MJP 3600 Series, 3D Systems).

Cartilage samples from the knee of an adult bovine were cut to fit the cartilage-hosting parts using a surgical instrument for bone/cartilage biopsies (Longueur) with an inner diameter of 6.4 mm. The cylindrical-shaped cartilage biopsies (diameter = 6.4 mm, length = 10 mm) were blocked between the cartilage-hosting parts by fitting them in the bottom part.

Figure 9c depicts the adhesion strength test steps. After performing the biopsy from bovine cartilage, the tissue was loaded and fixed within the cartilage-hosting parts, and the set-up was assembled. For testing the primers, 100 μ L of primer were poured on the sample. Then, 400 μ L of hydrogel were delivered and crosslinked. Immediately after hydrogel crosslinking, the hydrogel-hosting part was hooked to the load cell, and the test was performed in traction modality using a displacement speed of 1 mm min^{-1} until mechanical failure of the interface. Force curves as a function of the displacement were obtained from each tensile test, and the adhesion strength (in kPa) was determined by dividing the force by the

contact area between the hydrogel and the cartilage tissue. From each adhesion strength curve, the maximum adhesion strength (kPa) value was considered. Furthermore, the work of adhesion (in J m^{-2}) was obtained by considering the area under the load-displacement curve up to 1 mm of displacement divided by the hydrogel–cartilage tissue contact area.

A summary of the tested conditions for all primers and both GG and GGMA based hydrogels is reported in Figure 10.

For the FG, the two components were extruded simultaneously through a double-lumen tip provided by the FG supplier (Evicel Application Device) by applying manual pressure. In particular, 100 μ L of this primer were poured directly on the bovine knee cartilage, and different waiting times (30 s, 5 min, 15 min, or 30 min) were investigated (Figure 10a). Then, 400 μ L of GG or GGMA hydrogels were deposited onto the primer and crosslinked as described in Section 2.3.

For the primers containing CNFs, 100 μ L of CNF-laden GG- or GGMA-based adhesive layer were poured on the bovine knee cartilage and crosslinked for 10 min with MgCl_2 solution (1% w/v in $\text{d-H}_2\text{O}$) in the case of GG, or with a white LED source (intensity: 15 mW cm^{-2} , for 2.5 min) in the case of GGMA, before casting the respective hydrogel solution on top of it. Then, 400 μ L of GG or GGMA hydrogels were deposited and crosslinked for 10 min, as previously reported in the case of FG (Figure 10b).

For the CAT-based primer, either 100 mg mL^{-1} or 125 mg mL^{-1} of the CAT-modified gelatin was dissolved in tris buffered saline (TBS) (pH 7.4) solution containing 1×10^{-3} M Ru and 20×10^{-3} M SPS. Ru and SPS were prepared as 50×10^{-3} M and 1 M stock solutions in $\text{d-H}_2\text{O}$, respectively. 100 μ L of the CAT-modified gelatin solution were cast on the bovine knee cartilage and irradiated with a white LED lamp for 30 s (intensity: 15 mW cm^{-2}). Then, 400 μ L of GG or GGMA solutions were cast on top of the

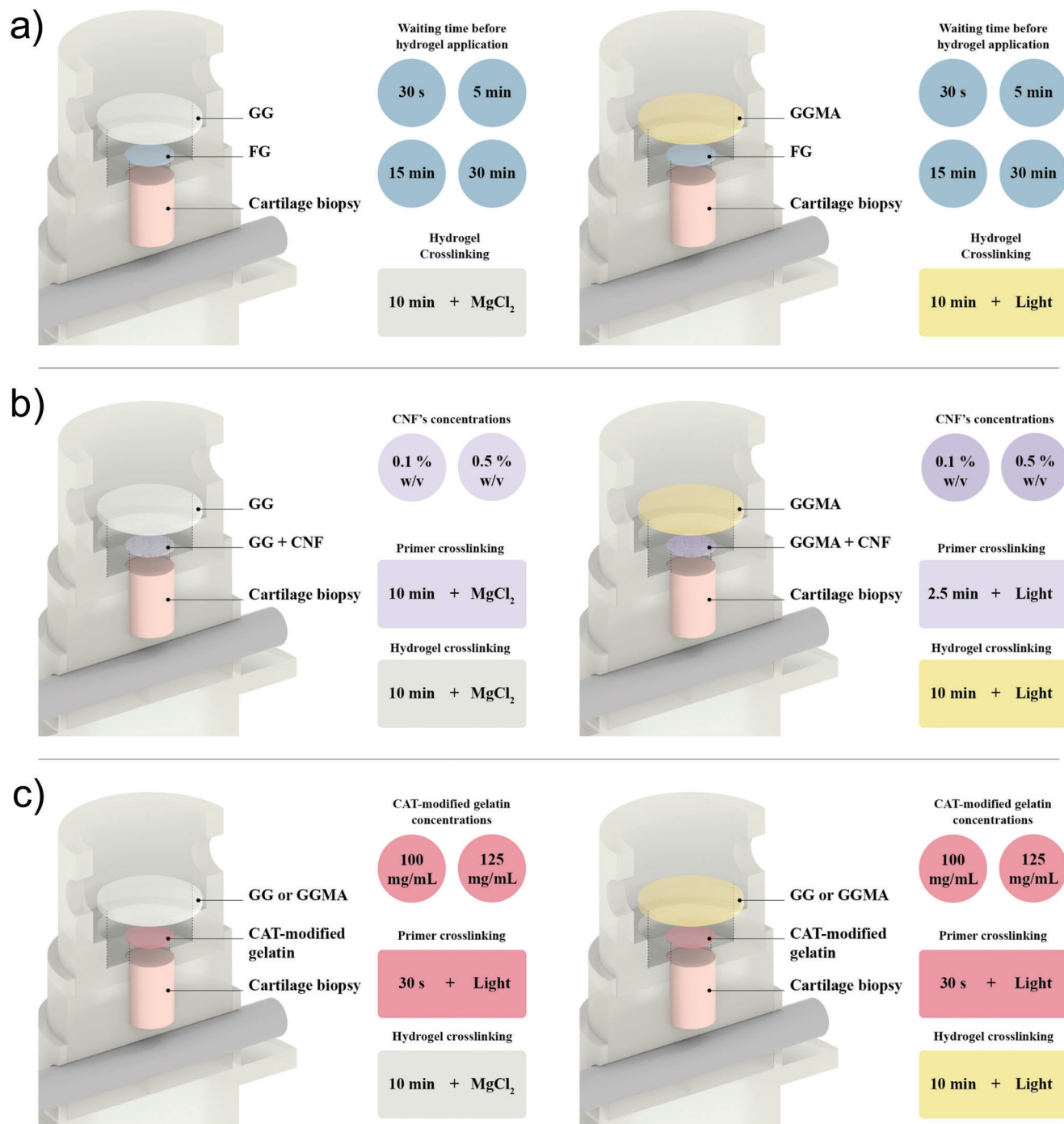


Figure 10. Depiction of the samples analyzed and the experimental conditions for applying a) FG, b) CNF-embedded GG and GGMA layers, and c) CAT-modified gelatin layers as primers. GG, gellan gum; GGMA, gellan gum methacrylated; FG, fibrin glue; CNF, cellulose nanofibers; CAT, catecholamines.

primer and crosslinked for 10 min, as previously reported in the case of FG and CNFs-laden layers (Figure 10c).

After performing the adhesion tests, representative images of all conditions were captured using 3D Digital Microscope HRX-01 (Hirox Europe, Limonest, France). Photos from a top and side view were acquired.

Biological Characterization of hASCs Encapsulated in Hydrogels: Cell viability, cytotoxicity, and metabolic activity of hASC encapsulated in GG and GGMA were analyzed after 2 and 7 d of culture.

Cell viability was evaluated using the Live/Dead kit (Life Technologies). Briefly, hydrogels were washed in D-PBS (Aurogene Srl) and incubated with the Live/Dead solution for 35 min at 37 °C. After staining, hydrogels were washed again with DPBS and visualized through a fluorescence microscope (Nikon Instruments Europe BW) to evaluate the live cells, stained in green, and the nuclei of dead cells, stained in red.

Cytotoxicity was assessed by using the LDH assay kit (Roche). The supernatants were collected after 2 and 7 d, and quantification was carried

out with a microplate reader (TECAN Infinite 200 PRO, Tecan Italia S.r.l.), setting absorbance at 490 nm.

Cell metabolic activity was analyzed through the Alamar blue test. Briefly, samples were incubated with 10% Alamar blue (Life Technologies); after 5 h, absorbance was read at 570 and 600 nm using an automated spectrophotometric plate reader (TECAN Infinite 200 PRO, Tecan Italia S.r.l.). The results were expressed as percentages of AlamarBlue reduction, as indicated by the manufacturer's data sheet (Biorad Laboratories).

Migration of hASCs toward the Hydrogels: To evaluate cell migration toward the hydrogels, 1×10^4 hASCs were seeded in 8 μm pore-sized HTS transwell polycarbonate insert systems (Corning). The two hydrogels (GG and GGMA) were placed in the lower chamber, and 150 μL of serum-free culture medium was added onto the insert. After 24 h, the hASCs migrated through the transwell on the lower surface of the membrane were gently washed twice with PBS and fixed by 4% paraformaldehyde for 30 min. The nonmigrated cells (on the upper surface of the membrane) were gently wiped off with cotton swabs and the membrane was stained using 1% crystal violet for 10 min. From each well, photographs were taken in various membrane areas by an inverted microscope. Then, to quantify cell migration toward the hydrogels, the crystal violet was dissolved using 10% acetic acid for 20 min, and absorbance was measured at 590 nm. Serum-free culture medium and 20% fetal bovine serum (FBS) were used as negative (CTR-) and positive (CTR+) controls, respectively.

Migration of hASCs outward the Hydrogels: To evaluate cell migration outward the hydrogel, the hydrogels encapsulating cells were placed in the transwell polycarbonate insert systems, and 150 μL of culture medium containing 20% of FBS (used as positive chemoattractant for the cells) were added. After 24 h, the cells migrated were analyzed as described in the previous section.

Statistical Analyses: A normality test (Shapiro–Wilk) was performed on all experimental data to assess the data distribution, which resulted normal in all cases. Results were expressed as mean \pm SD. Data analysis was performed using the unpaired *t*-tests to evaluate statistically significant differences between two group types under analysis, while ordinary one-way ANOVA with Tukey's post-hoc tests were adopted for multiple comparisons. For biological evaluations, we used Wilcoxon paired test. Results were expressed as mean \pm SD. Statistical analyses were carried out using GraphPad Prism (v 8.0.2). The significance threshold was set at 5% (* $p < 0.05$) and 1% (** $p < 0.01$).

Supporting Information

Supporting Information is available from the Wiley Online Library or from the author.

Acknowledgements

This work received funding from the European Union's Horizon 2020 research and innovation program, grant agreement No 814413, project AD-MAIORA (ADVanced nanocomposite MAterials fOR in situ treatment and ulTRAsound-mediated management of osteoarthritis).

Open Access Funding provided by Scuola Superiore Sant'Anna within the CRUI-CARE Agreement.

Conflict of Interest

The authors declare no conflict of interest.

Data Availability Statement

The data that support the findings of this study are available from the corresponding author upon reasonable request.

Keywords

adhesion strength, cartilage repair, catecholamines, cellulose nanofibers, fibrin glue, gellan gum, hydrogel adhesion, injectable hydrogels

Received: March 3, 2022

Revised: June 6, 2022

Published online:

- [1] C. D. O'Connell, C. Di Bella, F. Thompson, C. Augustine, S. Beirne, R. Cornock, C. J. Richards, J. Chung, S. Gambhir, Z. Yue, J. Bourke, B. Zhang, A. Taylor, A. Quigley, R. Kapsa, P. Choong, G. G. Wallace, *Biofabrication* **2016**, *8*, 015019.
- [2] M. Liu, X. Zeng, C. Ma, H. Yi, Z. Ali, X. Mou, S. Li, Y. Deng, N. He, *Bone Res.* **2017**, *5*, 17014.
- [3] C. Di Bella, S. Duchi, C. D. O'Connell, R. Blanchard, C. Augustine, Z. Yue, F. Thompson, C. Richards, S. Beirne, C. Onofrillo, S. H. Bauquier, S. D. Ryan, P. Pivonka, G. G. Wallace, P. F. Choong, *J. Tissue Eng. Regen. Med.* **2018**, *12*, 611.
- [4] S. H. Jeong, M. Kim, T. Y. Kim, H. Kim, J. H. Ju, S. K. Hahn, *ACS Appl. Bio Mater.* **2020**, *3*, 5040.
- [5] Y. Liao, Q. He, F. Zhou, J. Zhang, R. Liang, X. Yao, V. Bunpetch, J. Li, S. Zhang, H. Ouyang, *Polym. Rev.* **2020**, *60*, 203.
- [6] A. K. Gaharwar, I. Singh, A. Khademhosseini, *Nat. Rev. Mater.* **2020**, *5*, 686.
- [7] M. A. Bonifacio, A. Cochis, S. Cometa, A. Scalzone, P. Gentile, G. Procinio, S. Milano, A. C. Scalia, L. Rimondini, E. De Giglio, *Mater. Sci. Eng., C* **2020**, *108*, 110444.
- [8] J. Chen, J. Yang, Li Wang, X. Zhang, B. C. Heng, D.-A. Wang, Z. Ge, *Bioact. Mater.* **2021**, *6*, 1689.
- [9] D.-A. Wang, S. Varghese, B. Sharma, I. Strehin, S. Fermanian, J. Gorham, D. H. Fairbrother, B. Cascio, J. H. Elisseeff, *Nat. Mater.* **2007**, *6*, 385.
- [10] M. T. Matter, F. Starsich, M. Galli, M. Hilber, A. A. Schlegel, S. Bertazzo, S. E. Pratsinis, I. K. Herrmann, *Nanoscale* **2017**, *9*, 8418.
- [11] E. Öztürk, T. Stauber, C. Levinson, E. Cavalli, Ø. Arlov, M. Zenobi-Wong, *Biomed. Mater.* **2020**, *15*, 045019.
- [12] J. L. C. Van Susante, P. Buma, L. Schuman, G. N. Homminga, W. B. Van Den Berg, R. P. H. Veth, *Biomaterials* **1999**, *20*, 1167.
- [13] J. Yang, R. Bai, B. Chen, Z. Suo, *Adv. Funct. Mater.* **2020**, *30*, 1901693.
- [14] H. K. Kjaergard, U. S. Weis-Fogh, *Eur. Surgical Res.* **1994**, *26*, 273.
- [15] T. Dehne, R. Zehbe, J. P. Krüger, A. Petrova, R. Valbuena, M. Sittinger, H. Schubert, J. Ringe, *BMC Musculoskeletal Disord.* **2012**, *13*, 175.
- [16] P. Karami, C. S. Wyss, A. Khoushabi, A. Schmocker, M. Broome, C. Moser, P.-E. Bourban, D. P. Pioletti, *ACS Appl. Mater. Interfaces* **2018**, *10*, 38692.
- [17] S. J. Eichhorn, A. Dufresne, M. Aranguren, N. E. Marcovich, J. R. Capadona, S. J. Rowan, C. Weder, W. Thielemans, M. Roman, S. Renneckar, W. Gindl, S. Veigel, J. Keckes, H. Yano, K. Abe, M. Nogi, A. N. Nakagaito, A. Mangalam, J. Simonsen, A. S. Benight, A. Bismarck, L. A. Berglund, T. Peijs, *J. Mater. Sci.* **2010**, *45*, 1.
- [18] J. A. Killion, L. M. Geever, D. M. Devine, J. E. Kennedy, C. L. Higginbotham, *J. Mech. Behav. Biomed. Mater.* **2011**, *4*, 1219.
- [19] A. C. Borges, C. Eyholzer, F. Duc, P.-E. Bourban, P. Tingaut, T. Zimmermann, D. P. Pioletti, J.-A. E. Manson, *Acta Biomater.* **2011**, *7*, 3412.
- [20] Y. Liu, S. Cheong Ng, J. Yu, W.-B. Tsai, *Colloids Surf., B* **2019**, *174*, 316.
- [21] H. Yao, J. K. Xu, N. Y. Zheng, J. L. Wang, S. W. Mok, Y. W. Lee, L. Shi, J. Y. Wang, J. Yue, S. H. Yung, P. J. Hu, Y. C. Ruan, Y. F. Zhang, K. W. Ho, L. Qin, *Osteoarthritis Cartilage* **2019**, *27*, 1811.
- [22] D. R. Pereira, J. Silva-Correia, S. G. Caridade, J. T. Oliveira, R. A. Sousa, A. J. Salgado, J. M. Oliveira, J. F. Mano, N. Sousa, R. L. Reis, *Tissue Eng., Part C* **2011**, *17*, 961.

- [23] Z. Xu, Z. Li, S. Jiang, K. M. Bratlie, *ACS Omega* **2018**, *3*, 6998.
- [24] Y. Lu, X. Zhao, S. Fang, *Foods* **2019**, *8*, 31.
- [25] J. Silva-Correia, J. M. Oliveira, S. G. Caridade, J. T. Oliveira, R. A. Sousa, J. F. Mano, R. L. Reis, *J. Tissue Eng. Regener. Med.* **2011**, *5*, e97.
- [26] D. F. Coutinho, S. V. Sant, H. Shin, J. T. Oliveira, M. E. Gomes, N. M. Neves, A. Khademhosseini, R. L. Reis, *Biomaterials* **2010**, *31*, 7494.
- [27] D. A. Learmonth, P. M. Costa, T. R. Veloso, C. B. Cunha, M. P. Cautela, C. Correia, M. C. Vallejo, R. A. Sousa, *Biomater. Sci.* **2020**, *8*, 3697.
- [28] S. S. Chaurasia, R. Champakalakshmi, R. I. Angunawela, D. T. Tan, J. S. Mehta, *Trans. Vis. Sci. Technol.* **2012**, *1*, 2.
- [29] M. M. Domingues, F. L. Macrae, C. Duval, H. R. Mcpherson, K. I. Bridge, R. A. Ajjan, V. C. Ridger, S. D. Connell, H. Philippou, R. A. S. Ariens, *Blood* **2016**, *127*, 487.
- [30] K. S. Lim, B. J. Klotz, G. C. J. Lindberg, F. P. W. Melchels, G. J. Hooper, J. Malda, D. Gawlitta, T. B. F. Woodfield, *Macromol. Biosci.* **2019**, *19*, 1900098.
- [31] A. Narayanan, Y. Xu, A. Dhinojwala, A. Joy, *ChemEngineering* **2020**, *4*, 32.
- [32] A. H. Bacelar, J. Silva-Correia, J. M. Oliveira, R. L. Reis, *J. Mater. Chem. B* **2016**, *4*, 6164.